**Article ID:** 1003－6326(2003)05－1086－06

# Effects of load mode on mechanical properties of $ZrO_2$(2Y)/TRIP steel composites①

ZHOU Yu(周 玉)[1], GUO Ying-kui(郭英奎)[1, 2], LI Dong-bo(李冬波)[1], DUAN Xiao-ming(段小明)[1]
(1. School of Materials Science and Engineering, Harbin Institute of Technology, Harbin 150001, China;
2. School of Materials Science and Engineering,
Harbin University of Science and Technology, Harbin 150040, China)

**Abstract:** The $ZrO_2$(2Y)/TRIP steel composites were prepared by vacuum hot-pressing sintering. The room temperature static tensile and dynamic yield strength were tested using the static tensile and Split Hopkinson Pressure Bar methods, respectively. The effects of load mode on the static and dynamic mechanical behaviors were studied. The results show that the static tensile strengths of the composites decrease with the increase of $ZrO_2$ content, for the weak bonding of $ZrO_2$/$ZrO_2$. Under the dynamic load, the matrix TRIP steel produces the martinsitic phase transformation, which improves the dynamic strength and deformation ability of the composites. When the volume fraction of $ZrO_2$ exceeds 20%, the strain-hardening coefficient and the dynamic deformation ability of the composites decrease.

**Key words:** $ZrO_2$(2Y)/TRIP steel composite; static strength; dynamic strength; martinsitic phase transformation
**CLC number:** TG 386 **Document code:** A

## 1 INTRODUCTION

Armour materials bear the high-speed striking load. So it is beneficial to the ballistic properties of the materials by improving the absorbed energy under dynamic load or inducing the phase transformation strengthening during the absorbing energy process[1, 2]. Transformation induced plasticity steel (TRIP) has the good transformation plasticity, high room temperature static strength and good welding property and is a promising armour material[3, 4]. $ZrO_2$ has high strength, high hardness and good chemical consistent properties when it is compounded with steel[5, 6]. In the past, many researchers separately studied the static room temperature mechanical properties and stress-induced phase transformation of these two materials[7－10]. However, the dynamic mechanical properties and the properties of the composites comprised of these two materials have scarcely been reported. The present research is initiated to process a new $ZrO_2$(2Y)/TRIP steel composite and study the effect of $ZrO_2$ content on the static and dynamic mechanical properties of the composites.

## 2 EXPERIMENTAL

Partially stabilized zirconia (PSZ, 2% yttria, mole fraction), with the average grain size of 0.65 μm, was used as the raw material. Its composition is listed in Table 1. The XRD result shows that the powders consist of *t* phase(22%, volume fraction) and *m* phase(78%, volume fraction).

**Table 1** Chemical compositions of $ZrO_2$(2Y) powders (mass fraction, %)

| $ZrO_2$ | $Al_2O_3$ | $Y_2O_3$ | $SiO_2$ |
|---|---|---|---|
| 96.32 | < 0.02 | 3.60 | < 0.017 |
| $Fe_2O_3$ | $Na_2O$ | MgO | CaO |
| < 0.01 | < 0.01 | < 0.01 | < 0.01 |

TRIP steel powders were processed as follows: 20 grade steel powders were mixed with Cr-Fe, Mn-Fe, Mo-Fe and pure Ni according to Table 2. The mixture was then melted at 1 600 ℃ in a vacuum and poured into a bar of 35 mm in diameter after being deoxidized by B sand. Then the bar was atomized by nitrogen gas into steel powder with an average particle size about 40 μm. A series of composites were investigated in this study, whose composition is presented in Table 3. The $ZrO_2$ and TRIP steel powder were mixed in alcohol for 30 h, and then vacuum hot pressed after drying. According to our previous work, the sintering technique was determined as 1 250 ℃/1.7 × $10^{-1}$ Pa/20 MPa/30 min[11, 12], and the increasing temperature rate 20 ℃/min.

① **Received date:** 2002－10－22; **Accepted date:** 2003－03－24
**Correspondence:** GUO Ying-kui, PhD; Tel: +86-451-86414291; E-mail: ce921@hope.hit.edu.cn

**Table 2** Chemical compositions of TRIP steel powders (mass fraction, %)

| C | Cr | Mn | Ni | Mo | Si | Fe |
|---|---|---|---|---|---|---|
| < 0.18 | 8.50 | 1.10 | 4.50 | 3.70 | 1.70 | Bal. |

**Table 3** Compositions of composites (volume fraction, %)

| Type of composite | Composition of composite |
|---|---|
| TZ10 | TRIP steel+ 10% $ZrO_2$(2Y) |
| TZ15 | TRIP steel + 15% $ZrO_2$(2Y) |
| TZ20 | TRIP steel + 20% $ZrO_2$(2Y) |
| TZ25 | TRIP steel + 25% $ZrO_2$(2Y) |
| TZ30 | TRIP steel + 30% $ZrO_2$(2Y) |
| TZ35 | TRIP steel + 35% $ZrO_2$(2Y) |

The static tensile strengths of the composites were measured at the room temperature using Instron-5500 machine, with the crosshead rate of 0.5 mm/s, and the bar gauge is shown in Fig. 1. The dynamic mechanical properties of the composites were measured by Split Hopkinson Pressure Bar(SHPB) method, with the bar gauge of 6 mm × 6 mm × 6 mm and the strain rate of $2.5 \times 10^2$ $s^{-1}$. The schematic of Hopkinson experiment is shown in Fig. 2. And the fracture morphology of the composites was evaluated using SEM.

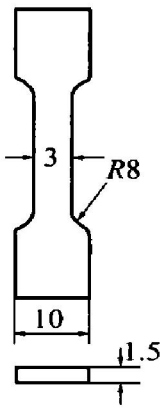


**Fig. 1** Bar gauge of specimen for static tension

## 3 RESULTS AND DISCCUSION

### 3.1 Static tensile strength of $ZrO_2$(2Y)/TRIP steel composites

Static tensile load—elongation curves of the $ZrO_2$(2Y)/TRIP steel composites are shown in Fig. 3. The straight trend of the data suggests that the composites characterize with brittle fracture under static tensile load. The dependences of elastic modulus and static tensile strength of the composites on the $ZrO_2$ content are shown in Fig. 4 and Fig. 5, respectively.

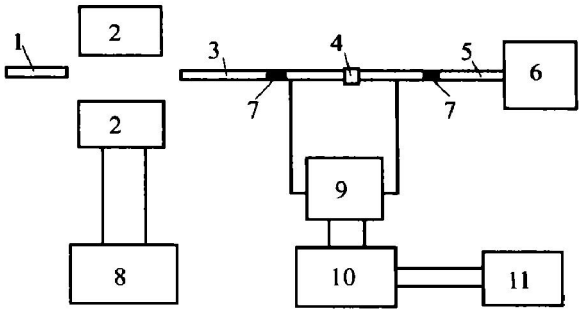


**Fig. 2** Schematic of SHPB test
1—Bullet; 2—System of velocity measurement; 3—Impact bar; 4—Sample; 5—Output bar; 6—Damper; 7—Strain gauge; 8—Wave from memory; 9—Super-dynamic gauge; 10—Digital oscilloscope; 11—Micro computer

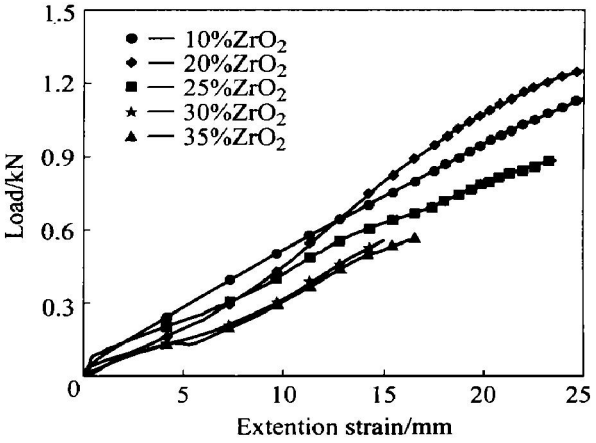


**Fig. 3** Relationship between load and extension strain of $ZrO_2$(2Y) TRIP steel composites

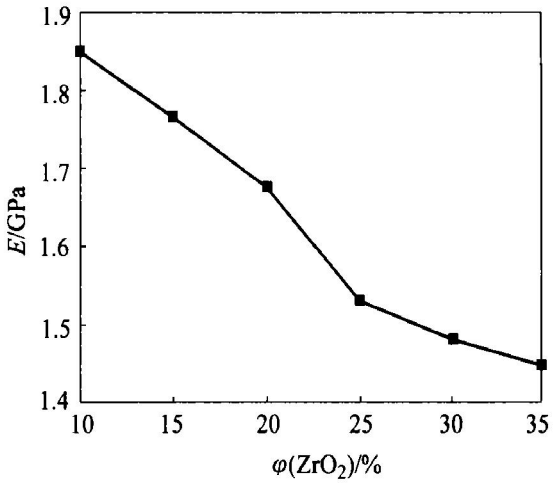


**Fig. 4** Elastic modulus of composites as function of $ZrO_2$ content

With the increase of $ZrO_2$ content, the tensile strength and the elastic modulus of the composites decrease monotonously. When the volume fraction of $ZrO_2$ changes from 10% to 35%, the strength and the elastic modulus of the composites decrease from 470 to 165 MPa, and from 1 850 to 1 350 MPa,

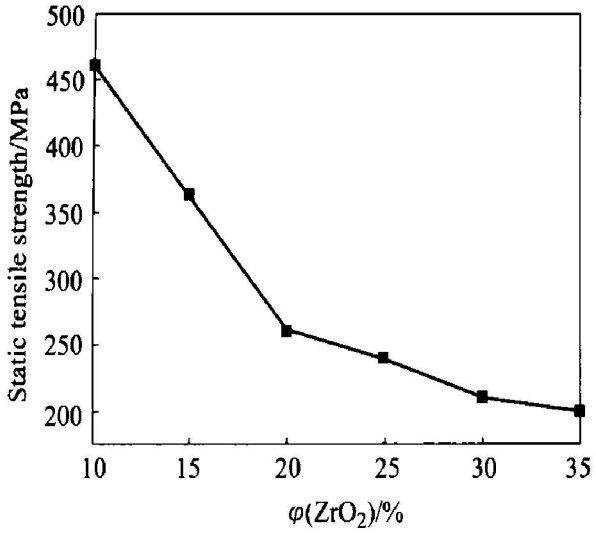


**Fig. 5** Static tensile strength of composites versus $ZrO_2$ content

respectively. The dependence of Vickers hardness of the composites on the $ZrO_2$ content is shown in Fig. 6, indicating that the hardness tested before and after tensile experiment show little variation and it only varies with the $ZrO_2$ content. It proves that no phase transformation is induced by the static tensile load in the $ZrO_2$(2Y)/TRIP steel composites.

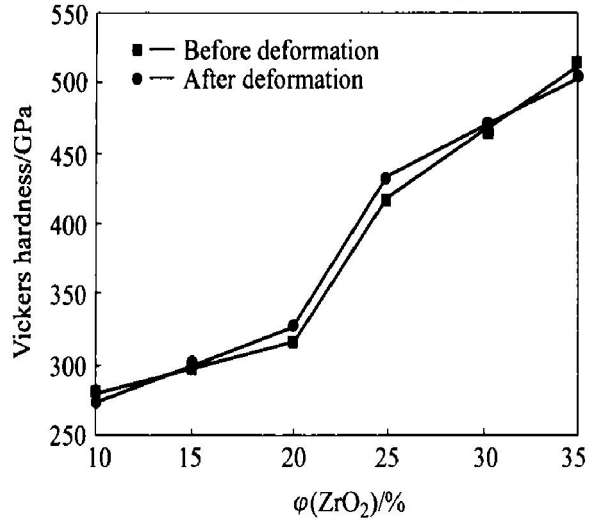


**Fig. 6** Vickers hardness of composites as function of $ZrO_2$ content

Under the static tensile load, the stress, strain as well as the deformation along the length of the samples are not uniform in the $ZrO_2$(2Y)/TRIP steel composites. The soft TRIP steel is deformed firstly, on the contrary, the $ZrO_2$ with high hardness is deformed a little. The deformation mismatch between $ZrO_2$ and TRIP steel leads to the high stress concentration at their interfaces, which increases with the increase of deformation of the TRIP steel. The stress concentration takes effect on the small zone of $ZrO_2$/TRIP interfaces and influences several layers of $ZrO_2$ particles near the interfaces. Due to the low sintering temperature, the strength of $ZrO_2$/$ZrO_2$ interfaces is lower than that of $ZrO_2$/TRIP ones. As a result, the crack initiates at the $ZrO_2$/$ZrO_2$ interfaces firstly, and then propagates when reaching the critical size, which finally results in the fracture of the composites. According to Smith's none uniform deformation model, the fracture stress is described as

$$\sigma = \sqrt{\frac{8(1+\upsilon)K_{IC}^2\gamma_c}{\pi C_0 E}} \quad (1)$$

In the 20% $ZrO_2$(2Y)/TRIP(volume fraction) steel composites, the value of $K_{IC}$ is 10.45 MPa·$m^{1/2}$, which is tested by the experiment, and the Poisson ratio $\upsilon$ is 0.3, and that of $\gamma_c$ is 3.5 J/$m^2$. The calculated fracture stress according to Eqn(1) is 277.99 MPa, which is near the tested value.

Fig. 7 shows the SEM micrographs of the fractural surface of the static tensile samples, which can verify the foregoing statement. It can be seen that the microcracks initiate at the $ZrO_2$/$ZrO_2$ interfaces. After ball milling, the average grain size of TRIP steel particles becomes smaller, but it is still much larger than that of $ZrO_2$ particles. As a result, the fine $ZrO_2$ particles distribute among the gaps of coarse TRIP steel particles and destroy the connectivity of the matrix in the composites. Due to the low sintering temperature (1 250 ℃), the bonding between the $ZrO_2$ particles is weak. When the applied stress is induced, the crack can easily propagate along the weak $ZrO_2$/$ZrO_2$ interfaces and can connect circling one or several TRIP particles. The weak bonding between particles finally leads to the brittle fracture of the composites. With the increase of $ZrO_2$ content, the weak $ZrO_2$/$ZrO_2$ interfaces increase, thus the tensile strength and elastic modulus of the composites decrease.

### 3.2 Dynamic yield strength of $ZrO_2$(2Y)/TRIP steel composites

Fig. 8 shows the dynamic stress—strain curves for $ZrO_2$(2Y)/TRIP steel composites. Compared with the static ones, the dynamic stress—strain curves consist of elastic-plastic and plastic deformation regions. Also, the composites show the evident dynamic yield. The dynamic yield strength of the composites increases with increasing $ZrO_2$ content up to 30% (volume fraction), then decreases. When the $ZrO_2$ content is 10% (volume fraction), the dynamic yield strength of the composites is 1 250 MPa, which is 2.5 times larger than the static tensile strength. It can be concluded that the load mode can efficiently take effect on the mechanical properties of the composites. The composites show the better deformation ability under the dynamic load than that under the static one.

Fig. 9 shows the impulse waveform of the

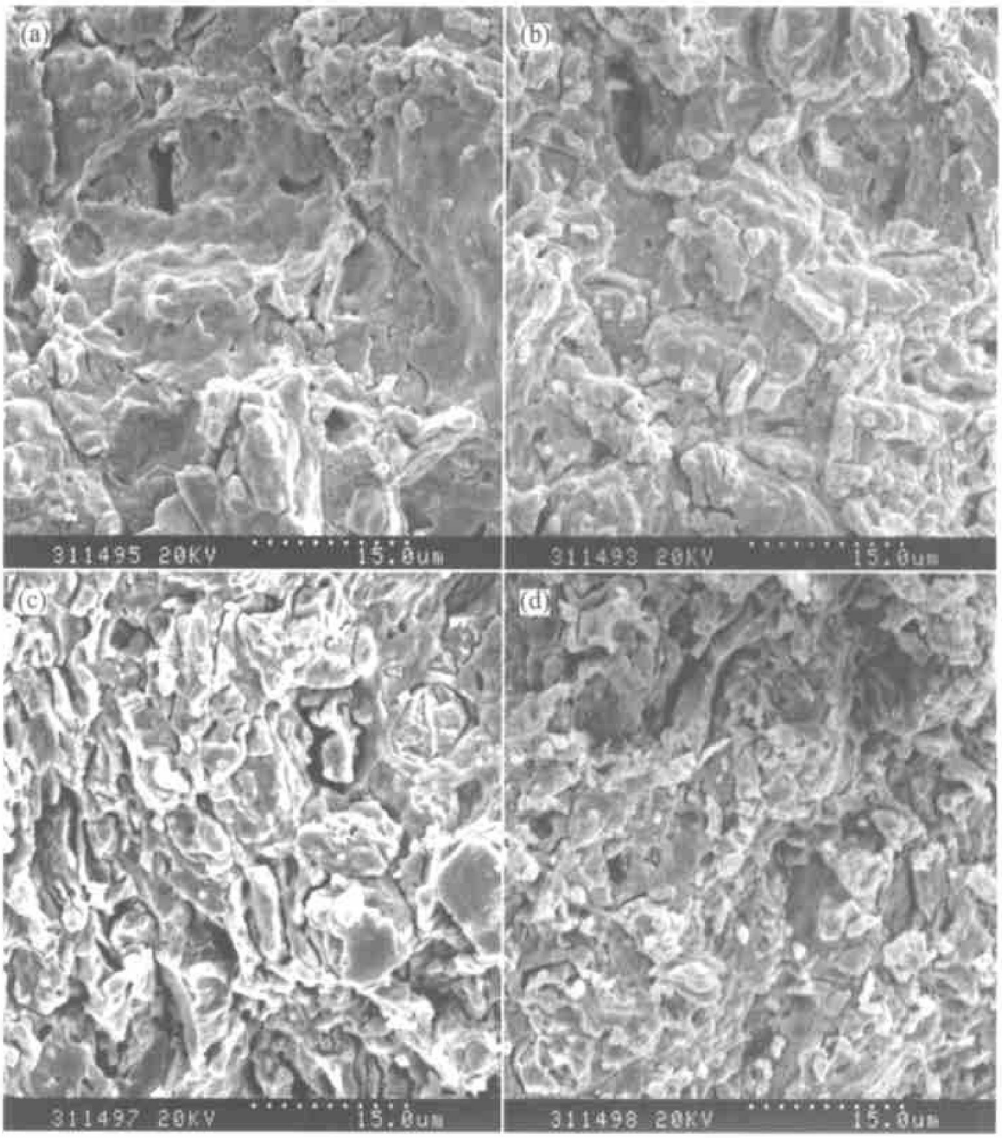


**Fig. 7** SEM fractographs of static tension of $ZrO_2$(2Y)/TRIP steel composites
(a) —TZ10; (b) —TZ20; (c) —TZ30; (d) —TZ35

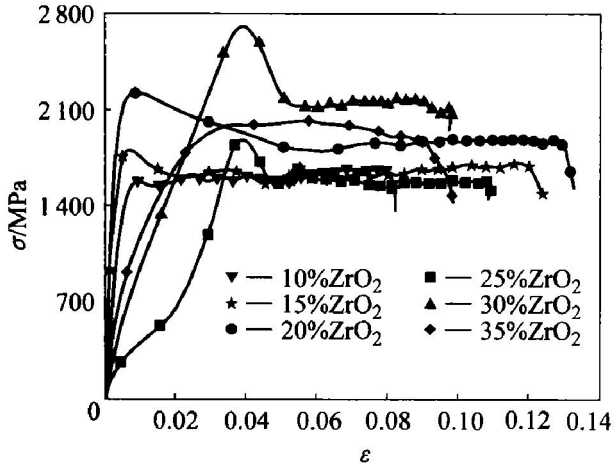


**Fig. 8** Dynamic stress—strain curves of $ZrO_2$(2Y)TRIP steel composites

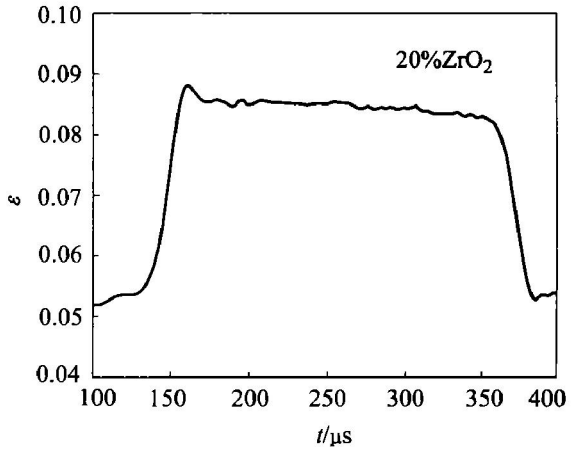


**Fig. 9** Wave figure of SHPB input bar

input bar. The propagation velocity of the stress wave $U = \sqrt{\frac{\rho}{E}}$ is so fast and the specimens are so small that the stress can reach a balance in a short time and can be processed by the quasi-static method. Fitting the curves in Fig. 8 by the traditional Hollomon Eqn(2) and then taking the logarithm of Eqn(2) yields a new Eqn(3):

$$\sigma = A\varepsilon^{n_1} \tag{2}$$

$$\ln \sigma = \ln A + n_1 \ln \varepsilon \quad (3)$$

where $A$ is strength coefficient, and $n_1$ is the strain-hardening coefficient. Fig. 10 shows the relationship between $\ln \sigma$ and $\ln \varepsilon$, where $\ln \sigma$ and $\ln \varepsilon$ are dynamic stress and strain of the composites, respectively. It can be seen that the $n_1$ values of every curves are equal at the beginning of the deformation, so the $ZrO_2$ content takes little effect on the strain-hardening coefficient. By least square method calculating, the 10% $ZrO_2$(2Y)/TRIP steel composite has $n_1$ value of 0.235, which is equal to that of normal steel. It can be concluded that the deformation ability of $ZrO_2$(2Y)/TRIP steel composite mainly depends on the matrix of TRIP steel. Seen from the evident double-wave figure of the transmission wave (Fig. 11), the matensitic phase transformation takes place in the TRIP steel under the dynamic load referring to Fig. 12. In Fig. 12, both Fig. 12(a) and Fig. 12(b) are distortion induced martensites and theirs substructures are twin caused by inhomogeneous distortion after adding $ZrO_2$ into them. This phase transformation couples the plastic deformation, which relaxes the stress concentration, increases

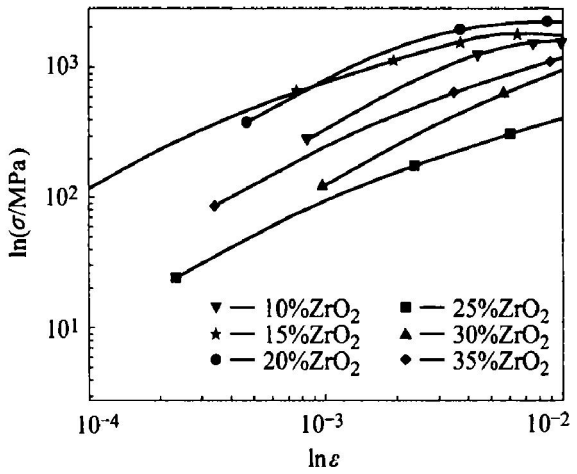


**Fig. 10** Relationship between $\ln \sigma$ and $\ln \varepsilon$ of composites

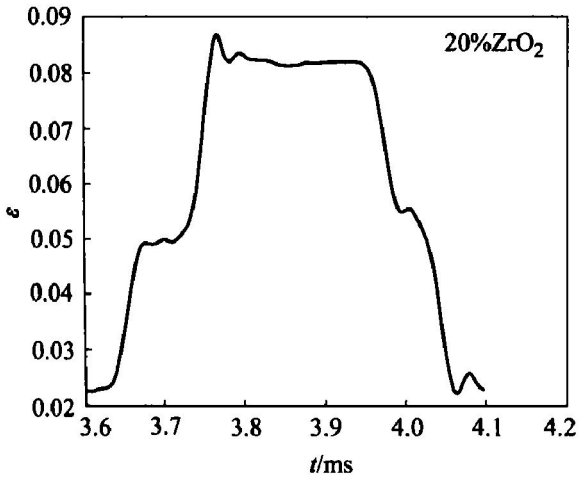


**Fig. 11** Wave figure of SHPB output bar

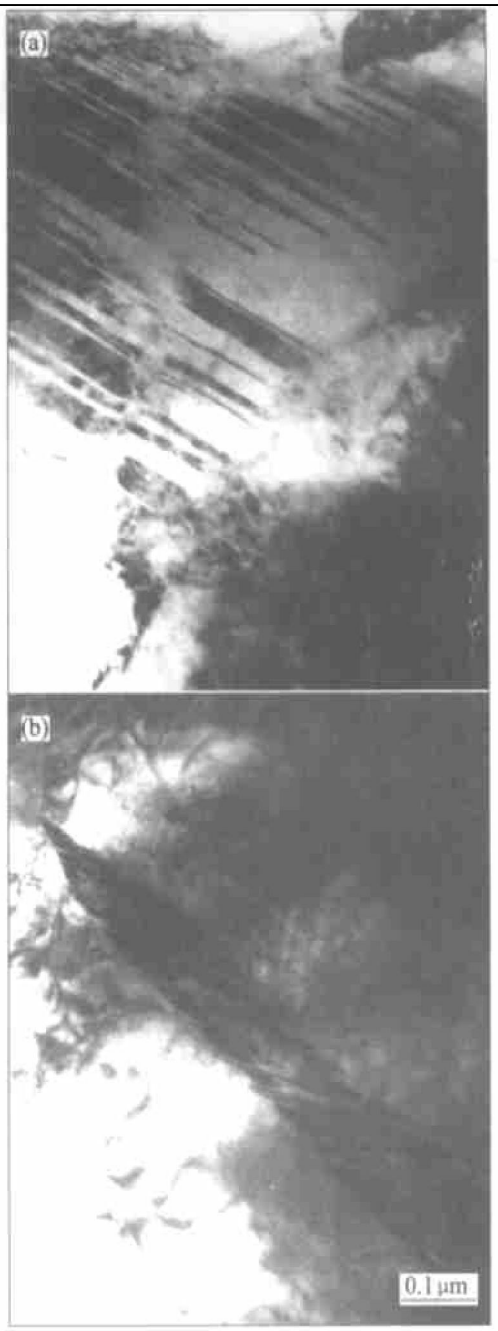


**Fig. 12** TEM images of $ZrO_2$(2Y)/TRIP steel composites under dynamic load
(a) —TZ20; (b) —TZ25

the deformation ability, and prevents the fracture under small strain. In addition, it induces the further deformation strengthening and increases the dynamic strength of the composites. With the increase of deformation, the effect of $ZrO_2$ on the value of $n_1$ becomes evident. Seen from Fig. 10, the value of $n_1$ decrease slowly with the increase of $ZrO_2$ content. It is because $ZrO_2$ prevents the deformation of the TRIP steel matrix. The increase of $ZrO_2$ improves the rheological stress and increases the fracture strength of the composites, but on the other hand it prevents the martinsitic phase transformation, and therefore prevents the deformation of the TRIP steel matrix. When the volume fraction of $ZrO_2$ exceeds 20%, the deformation ability of the composites de-

creases, leading to the decrease of the fracture strength. Taking account of the effect of $ZrO_2$ content on the martinsitic phase transformation of the TRIP steel matrix and the resulted deformation of the composites, Eqn(2) can be changed to:

$$\sigma = (1 - x) A \varepsilon^n \quad (4)$$

where $x$ represents the $ZrO_2$ content. After coupling, it is described as $\sigma = 2\,881.310(1 - x)\varepsilon^{0.235}$, which favorably corresponds with the real curves.

## 4 CONCLUSIONS

1) Under the static load, tensile strength and elastic modulus of $ZrO_2$(2Y)/TRIP steel composites decrease with the increase of $ZrO_2$ content, which is caused by the weak bonding of $ZrO_2/ZrO_2$ particles and $ZrO_2$/TRIP steel particles.

2) Under the dynamic load, the relationship between stress and strain in $ZrO_2$(2Y)/TRIP steel composites can be described by the equation: $\sigma = 2\,881.310(1 - x)\varepsilon^{0.235}$. The dynamic yield strengths of the composites are larger than the static tensile ones because of the martinsitic phase transformation, which further couples the plasticity and finally improves the deformation ability of the composites.

3) At the beginning of the dynamic deformation, the effect of $ZrO_2$ content on deformation strength of the composites is not evident. The rheological stress in the $ZrO_2$(2Y)/TRIP steel composites increases with the increase of $ZrO_2$ content and deformation. However, when the volume fraction of $ZrO_2$ exceeds 30%, the deformation ability and dynamic fracture strength of the composites decrease.

## REFERENCES

[1] CHEN Mao-ai, WU Chuan-song, GAO Jin-qiang. Welding of SiC particle reinforced 6061 Al matrix composite with pulsed TIG[J]. Trans Nonferrous Met Soc China, 2002, 12(5): 805-810.

[2] WANG Xiang, ZENG Song-yan, SONG Run-bin, et al. Dry sliding friction and wear behaviors of TiC/2A-12 composites[J]. Trans Nonferrous Met Soc China, 2002, 12(3): 419-423.

[3] Fischer F D, Reisner G, Werner E, et al. A new view on transformation induced plasticity (TRIP)[J]. Inter J Plasticity, 2000, 16: 723-748.

[4] Jung Y D, Choi S C, Oh C S. Residual stress and thermal properties of zirconia/metal(nickel, stainless steel 304) functionally gradient materials fabricated by hot pressing[J]. J Mater Sci, 1997, 32: 3841-3850.

[5] ZHOU Y. Ceramic Materials[M]. Harbin: Harbin Institute of Technology Press, 1996. 35-50. (in Chinese)

[6] Jung Y G, Paik U, Choi S C. Influence of the particle size and phase type of zirconia on the fabrication residual stress of zirconia/stainless-steel 304 functionally gradient material[J]. J Mater Sci, 1999, 34: 5407-5416.

[7] Li Z G, Minoru Taya, Dunn M I. Experimental study of the fracture toughness of a ceramic/ceramic-matrix composite sandwich structure[J]. J American Cera Soc, 1995, 32(3): 1633-1639.

[8] XU Zu-yao. Martensite and Martensitic Phase Transformation[M]. Science Press, 1999. 693-695. (in Chinese)

[9] Liang K M, Gu K F, Fantozzi G. Mechanical analysis of indentation cracking for transformation toughening ceramics[J]. J Chinese Cera Soc, 1994, 22(1): 29-37. (in Chinese)

[10] Kang Y L, Wang B. Structure and property of TRIP plate and its control process[J]. J Iron and Steel Res, 1999, 11(3): 62-66. (in Chinese)

[11] Zhao M, Guo Y K, Yu Z M, et al. Effect of sintering temperature on the density and strength of stainless steel (316)[J]. J Harbin Univ of Sci and Technol, 2000, 5(3): 105-107. (in Chinese)

[12] LI D B. Microstructure and Mechanical Properties of $ZrO_2$/316L Stainless Steel Composites[D]. Harbin: Harbin Institute of Technology, 1999. 16-18. (in Chinese)

(Edited by CHEN Wei-ping)